

# Pulsed Nd:YAG Laser Treatment for Failing Dental Implants Due to Peri-implantitis.

Dawn Nicholson<sup>a</sup>, Kris Blodgett<sup>b</sup>, Beaverton, OR; Charles Braga<sup>b</sup>, Newmarket, NH;  
Larry Finkbeiner<sup>b</sup>, Colorado Springs, CO; Jeanne Fourrier<sup>b</sup>, Surfside Beach, SC;  
John George<sup>b</sup>, Pittsfield, MA; Robert Gregg, II<sup>a</sup>; Allen Honigman<sup>b</sup>, Gilbert, AZ;  
Bruce Houser<sup>b</sup>, Scottsdale, AZ; William Lamas<sup>b</sup>, Miami, FL; Neal Lehrman<sup>b</sup>, New York, NY;  
Eric Linden<sup>b</sup>, Woodcliff Lake, NJ; Delwin McCarthy<sup>a</sup>, Tom McCawley<sup>b</sup>, Ft. Lauderdale, FL;  
Randy McCormick<sup>b</sup>, Tulsa, OK; Ed Marcus<sup>b</sup>, Yardley, PA; Kirk Noraian<sup>b</sup>, Bloomington, IL;  
Peter Rubelman<sup>b</sup>, N. Miami Beach, FL; Maurice Salama<sup>b</sup>, Atlanta, GA;  
Steve Saunders<sup>b</sup>, Harrisonburg, VA; Brandon Seamons<sup>b</sup>, Honolulu, HI;  
David Thein<sup>b</sup>, Overland Park, KS; Michael Toms<sup>b</sup>, Cincinnati, OH; George Vassos<sup>b</sup> Agawam, MA;  
David M. Harris<sup>c</sup>

- a. Institute for Advanced Laser Dentistry, Cerritos, CA 90703
- b. Private Dental Practice
- c. Bio-Medical Consultants & Associates, Inc., Paradise CA 95969

## ABSTRACT

A large percentage of dental implants experience complications, most commonly, infection leading to peri-implantitis and peri-mucositis, inflammatory disease involving pathogen contamination. It presents with radiographic findings of crestal bone loss. At this time there appears to be no compelling evidence for an effective intervention. The LANAP protocol is a FDA cleared surgical protocol that produces new attachment and bone regeneration when applied to periodontally infected natural teeth. The LANAP protocol and laser dosimetry have been modified to treat ailing and failing implants. Twenty-one clinicians who have been trained to perform the LANAP protocol and the LAPIP™ protocol have volunteered 26 LAPIP case reports. The time from implant to intervention ranges from 3 months to 16 years. Post-LAPIP radiographs range from 2-48 months. Ten cases were excluded for technical reasons. All 16 remaining cases provide radiographic evidence of increase in crestal bone mass around the implant and, when reported, probe depth reductions. All treating clinicians report control of the infection, reversal of bone loss and rescue of the incumbent implant. Although the success/failure rate cannot be judged from these data, any successes in this area deserve reporting and further study.

Key words: Pulsed Nd:YAG laser, dental laser, dental implant, LANAP, periodontal infection, peri-implantitis.

## INTRODUCTION

We introduce a new indication for the application of the pulsed Nd:YAG laser for the successful treatment of the infectious disease, peri-implantitis and peri-mucositis. Pilot data are presented in the form of 16 clinical case reports that provide radiographic evidence of immediate disease reversal and gradual bone regeneration following treatment with the LAPIP protocol.

Figure 1(a) [upper left] shows the relationship between a natural tooth (#8) in 2003 and its replacement with a dental implant in 2004. After six years the implant has developed shadows (radiolucencies) on the radiograph indicating bone loss around the coronal edge of the anchor, a primary indication for peri-implantitis. Peri-implantitis is an inflammatory disease in the bone and soft tissues that surround a dental implant. The tissues are colonized by pathogenic bacteria that gradually cause the degeneration of the alveolar bone that holds the implant in place<sup>1,2</sup> Progression of the disease will result in loss of the implant.

Reporting of implant complication rates varies between 11% – 56% of all implants.<sup>3,4</sup> It is estimated that annually about 1,000,000 dental implants are removed worldwide.<sup>5</sup> The most common risk factor seems to be advanced periodontitis on prior or missing teeth.<sup>6,7</sup> Current treatment options both surgical and non-surgical have at the most a 50-60% success rate<sup>8</sup> and there appears to be no clear evidence to identify the most effective method of treatment nor is there a standard protocol for management of this inflammatory process.

**LANAP protocol.** The LANAP protocol is a well defined step-by-step, minimally invasive, surgical procedure for treating periodontitis that requires training & proficiency certification on the 6 Watt PerioLase<sup>®</sup>MVP-7<sup>™</sup> FR pulsed Nd:YAG laser and licensure to perform the LANAP protocol. The entire protocol is accomplished with laser, piezo-ultrasonic and hand instrumentation and a dental handpiece but without scalpel, sutures or graft material.<sup>9-12</sup> LANAP therapy for periodontitis results in reattachment of natural teeth to the bone thru regeneration of the periodontal ligament and formation of new bone. The native structure of the attachment of dentition is actually regenerated.<sup>13-15</sup>

**LAPIP protocol.** The LANAP protocol was modified to treat peri-implantitis and peri-mucositis. The modified protocol is referred to as the LAPIP protocol). It is also a step-by-step surgery that requires training certification and licensure. The protocol follows the LANAP protocol sequence where appropriate.

We have conducted this study in preparation to running a clinical trial to establish the efficacy of the LAPIP protocol. Before/after radiographs from 26 LAPIP case reports with a successful response to treatment were submitted by 21 dentists in private practices. The time course of the response to treatment is determined from radiographic evidence. A model is developed to estimate the rate of crestal bone deposition following this laser assisted peri-implantitis procedure. Reports were also examined to identify issues for consideration in designing inclusion/exclusion criteria.

## METHODS

**Laser instrumentation.** The 6 Watt PerioLase<sup>®</sup>MVP-7<sup>™</sup> FR pulsed Nd:YAG laser was designed by dentists for use by dentists. The ergonomics and output parameters are optimized for each dental application. Pulse duration can be changed in 7 increments to go from cutting to hemostasis. The ranges of other parameters are also defined in terms of tissue response. Microprocessor based controls remember and recall the parameter set for specific tasks. The procedure presets are visible and parameters can be adjusted by the clinician within the limits of biologic tolerance. The delivery handpiece and tips are adjustable for access to all pockets. Feedback informs the user of the exact energy light dose and energy density being delivered. As the LANAP and LAPIP procedures evolve, so does the laser and vice-versa. The hardware and procedure have become closely integrated.

The LAPIP protocol specifies application of laser energy around ailing and failing implants in a similar way as the LANAP protocol applies energy around natural dentition. In both instances, device specific training and accumulated clinical judgment needs to be applied to adjust preset parameters and total dosimetry that is appropriate to the specific clinical presentation. In LAPIP the light dose used around implants is approximately one third the energy applied around natural teeth, primarily due to less dissipation of heat in implants and the greater fragility of the tissue surrounding them.

The LAPIP protocol generally follows the same steps with the same medical devices as the LANAP protocol with adjusted dosimetry. Currently, this laser assisted new attachment procedure uses the laser in the protocol to achieve the following objectives: laser bacterial reduction, selective photothermal ablation of pocket epithelium, laser hemostasis, photo-biomodulation, immune activation, tissue stabilization through formation of a durable fibrin gel clot. LANAP is a medical treatment protocol that utilizes the laser, the piezo ultrasonic scaler and special hand instrumentation.

**Radiographic analysis. Pilot study to develop methods for measurements.** All images were received as scanned and emailed digital reproductions of a series of at least two bitewing radiographs. One case was submitted as a CT scan of the mandible. Images were rotated, cropped and resized, if necessary, to form the sequential composites as shown in the figures. Brightness and contrast were not adjusted.

In the top row of Figure 1 the radiographs have been arranged in chronological order so that the reader can easily visualize the progression from natural tooth, to implant, to development of a lesion and the gradual diminishing of the peri-implant radiolucency following treatment.

The human eye/brain is excellent at discriminating objects from background and for identifying what has changed from one panel to the next. To capture and quantify this sequence a technician, skilled at reading dental radiographs, has identified the baseline alveolar crest (Figure 1(b) [04-28-2004, bottom]) and outlined the “areas of changes in radiolucencies” in subsequent images. A relatively easy task for the eye/brain but influenced by subjective bias. In order to be more objective we identify a criteria gray-level to define the boundary of the lesion. With these retrospective data this level is different for each case and may even vary from one visit to the next. This source of variance can be eliminated for a prospective clinical trial with controlled exposures and a computer-based algorithm. As an example, the clusters of green pixels (Figure 1(d)) represent pixels with a grey-level value that, in this case, defines the boundary criteria for the edge of the lesion. The lesion boundary is also defined by the baseline alveolar crest, the edge of the implant and for large defects the edge of the adjacent tooth. As a check for bias the aligned and outlined images were returned to investigators for their concurrence.

In some cases two processes appear evident in the radiographs (Figures 2 and 3). Dark shadows within the crestal bone are assumed to represent bone loss resulting in decreased radiodensity. Completely black areas are assumed to represent the absence of bone. Two contours are drawn; one for the black area (B) and a larger zone is outlined for the “shadow” (A).

Once the outlines are drawn it is a simple matter to measure the cross-sectional area of the lesion using public domain software (image J). Since the exact diameter and length of the implant are known the areas can be measured in  $\text{mm}^2$  and comparisons can be made across cases. The sum of the peri-implant areas on both sides of the implant is referred to in the figures as the cross-sectional area. For calculation of the volume of the lesion the cross-sectional area is the average of the right and left areas. The rate of recovery for each lesion is calculated as the difference in area between before and after lesions divided by the follow-up period.

## RESULTS

**Study population.** Twenty-one dentists contributed 26 LAPIP cases including before/after radiographs. Ten of the cases were excluded from analysis because: (1) The “after” radiograph was rotated relative to the “before” presenting a foreshortened or different cross-section. (2) Missing data (e.g., date of follow-up) and (3) the lesion extended beyond the image margins.

The remaining 16 cases included 9 females and 7 males with an average age of 54 years (range: 32-79). The median time that had elapsed between the date of implant and the date of treatment was 4 years with a range of 3 months to 16 years. Follow-up data ranged from 8 to 36 months post-LAPIP.

**Lesion progression and LAPIP intervention.** The two cases shown in Figure 4 illustrate the entire time course including development of the lesion, an immediate response to treatment and almost complete recovery. At the top is the case of Dr. Blodgett. Soon after implant a lesion developed on the left side, a year later the lesion encircled the post and continues to grow. The growth rate is closely approximated with an exponential function. LAPIP intervention is followed by a decrease in the size of the lesion. A similar sequence is seen at the bottom in a case submitted by Dr. Noraian. The total area of the lesion at each time point was measured. The results are plotted in (C) as total cross-sectional area (right plus left) VS time of follow up relative to LAPIP. The two cases have dramatically different infection growth rates, one five times the rate of the other. However, both lesions appear to heal at about the same rate.

**An unusual and interesting case of Dr. Neal Lehrman [Figure 5].** In June of 2007 an implant was placed in a 74 year old male at the site of #24. The patient was followed for 2 years without incident until he presented for an emergency visit and complained that the implant was loose. In fact, it was so loose that I was certain that I could easily remove and reinsert the entire fixture with just my fingers.

Periapical films made it clear that the case was failing (Figure 5). He was advised that the fixture should be extracted and grafted and then upon healing his options would be re-visited. He insisted that he needed to retain the implant for cosmetic purposes. So we discussed the laser treatment and, at the patient's request, LAPIP was performed around the fixture. I reasoned that there was minimal risk and at least we would remove the infection from the site. A bit of composite was used to splint it temporarily to the adjacent teeth. No antibiotics were used at this time.

Within a week the tissue started to resolve. There was no mobility since the splint was in place and the tooth was out of occlusion. At 7 months improvement was noted, radiographically (Figure 5), and the splint was re-bonded. At 18 months the bonding had disappeared and the patient had forgotten about the problem with the implant. Probing depths were within normal limits. There was little mobility, and no exudate from around the implant.

**Rate of recovery following LAPIP.** Recovery functions for all 16 cases are plotted in Figure 6. In those case with multiple time points there is a trend for recovery to slow over time. Consistent with this observation, it appears as if larger lesions heal faster. We computed a linear regression for the first segment of these functions to find the slope. This defines an initial rate of recovery (decrease in cross-sectional area) for each case. Rates ranged from 0.1 to 2.4 mm<sup>2</sup>/month with a mean rate of 1.24 mm<sup>2</sup>/month or 15 mm<sup>2</sup>/year. Complete recovery takes 1-3 years depending on the initial size of the lesion. Figure 7 shows the recovery rates for all cases relative to their original lesion size. There is a definite trend for larger lesions to heal faster. The correlation coefficient comparing initial size and rate is 0.69.

In two cases we measured only the decrease in the black zone assumed to be addition of bone to the alveolar crest (Figure 2, 3). The two values, 0.107 and 0.793 mm<sup>2</sup>/month appear to be a bit slower than recovery of bone density. In the discussion we will use these values along with a 3-D reconstruction to estimate the rate at which new crestal bone is forming.

## DISCUSSION

We have observed in our clinical practices some excellent results from applying the LAPIP protocol to cases of peri-implantitis. There is no doubt that what is presented here are some of the best cases “cherry picked” among the so-so responders and the failures. Yet, the two cases where we have historical data prior to LAPIP (Figure 4) clearly show an increasing zone of peri-implant bone loss due to the exponential growth of the infection. This growth is immediately halted and is followed by a continuous period of bone regeneration lasting up to three years post-treatment. In these cases applying the LAPIP protocol had an obvious cause-effect relationship. The other 14 cases also show regeneration over a range of rates following LAPIP.

The purpose of this survey was to examine and document the positive response to therapy and to try to identify the commonality to these cases that made them successful. We have also developed some techniques for data collection and analysis and estimated a time course for the response. These data will help define the inclusion/exclusion criteria and other considerations for the design of a clinical trial.

**The volume of the lesion can be estimated from the area of the cross-sectional profile.** One case provided as a CT scan allows a 3-dimensional view of a typical bony defect in peri-implantitis (Figure 8). The horizontal section indicates circular symmetry and is consistent with the assumptions of a geometric model. The well defined formula of the model is used to estimate the approximate volume of the lesion (Figure 9).

Peri-implantitis is an infection that typically encircles the coronal aspect of the implant anchor and grows to eventually encompass the apex. In Figure 8 the 3-dimensional shape of the lesion is approximated by a torus (donut). We can then use the known formula to estimate the actual volume from the cross-sectional area and the circumference of the torus. The model will tend to overestimate the actual volumes due to thinner bone that often forms the facial and lingual aspects of the bony socket. Knowing the volume is required for an accurate calculation of dosimetry. The geometry model and its change over time will be applied within our computer-based simulations of light distribution and “kill zones” for the LAPIP application.<sup>16,17</sup>

We also use this geometric model to estimate the rate of addition of new bone to the alveolar crest (Figure 9). The volume of a torus is equal to the circumference of the torus ( $2\pi R$ ) times its cross-sectional area ( $\pi r^2$ ). For the actual

lesion in Figure 9,  $R = 2.95$  mm and the cross-sectional area, the average of right and left areas, is  $= 2.09$  mm<sup>2</sup>. The volume of the lesion at 6 months is 38.7 mm<sup>3</sup>. Twelve months prior, at the time of intervention, the shape of the lesion was not a torus but this calculation still provides a reasonable estimate of the initial lesion volume which was 158 mm<sup>3</sup>.

**The rate of recovery decreases as the defect gets smaller.** It can be gleaned from Figures 6 and 7 that healing (bone deposition) following LAPIP in these cases is apparently not linear. For large defects it is rapid at first, but gradually slows as the defect disappears. This is represented by the dotted line which is an exponential fit to all data points (Figure 6).

**The rate of bone deposition can also be estimated.** It is assumed that changes in radiolucency represent changes in bone density. Furthermore the change in black peri-implant areas is assumed to relate to the absence of bone. A trained observer must be able to “mentally subtract” variations in radiolucency due to soft tissue shadows and other artifacts when outlining the lesions.

The 3-D model was applied to the “B” contour data from cases shown in Figures 2 and 3. The diameter of the torus is estimated to be 5.2 mm and 6.0 mm and the changes in volumes are calculated to be 1.6 mm<sup>3</sup>/month and 0.62 mm<sup>3</sup>/mo, respectively. These initial rates probably continue but gradually decline. This range of values may indicate specific physical regenerative processes that are involved in the healing event initiated by the LAPIP protocol.

**Efficacy of LAPIP. Conclusions from this survey should be generalized with caution.** In Figure 1 one can follow the entire progression of destruction, LAPIP intervention and reconstruction. When it works the LAPIP protocol apparently results in a steady reconstitution of the alveolar bone destroyed by the peri-implant infection. All treating clinicians report for these cases control of the infection, reversal of bone loss and rescue of the incumbent implant. We realize that these cases are among the best results to LAPIP therapy. Although the success/failure rate cannot be judged from these data, any successes in this area deserve reporting and further study.

## CONCLUSIONS

Disease progression appears to be exponential. LAPIP intervention caused disease reversal in these 16 cases. Healing following LAPIP for failing implants is continuous and occurs over a time span of 1-3 years, dependent on the initial lesion size.

Rate of recovery is about 15 mm<sup>2</sup> in cross-sectional area / year. In two cases new bone was added to alveolar crest at an approximate rate of 0.62 mm<sup>3</sup>/mo and 1.6 mm<sup>3</sup>/mo.

Radiographic data from these cases support the likelihood that LAPIP therapy initiated a healing event that continued for up to three years. This event reversed the disease process and continued to restore the bone mass that was destroyed by the infection.

## ACKNOWLEDGEMENTS

This study was supported by Millennium Dental Technologies, Inc., Cerritos, CA. David Harris and Bio-Medical Consultants received consulting fees from Millennium for their work on this project. Dawn Nicholson, Robert Gregg and Delwin McCarthy are Principals of Millenium. The other authors have no financial interest in the outcome of this study.

## REFERENCES CITED

- [1] Hultin, M, Gustafsson, A, Hallström, H, Johansson, LA, Ekfeldt, A, Klinge, B, “Microbiological findings and host response in patients with peri-implantitis,” Clin. Oral. Implants Res., 13(4), 349-58 (2002).
- [2] Papaioannou, W, Quirynen, M, Van Steenberghe, D, “The influence of periodontitis on the subgingival flora around implants in partially edentulous patients,” Clin Oral Implants Res., 7(4), 405-409 (1996).
- [3] Algraffee, H, Borumandi, F, Cascarini, L, “Peri-implantitis,” Br J Oral Maxillofac Surg, 50(8), 689-694 (2012).

- [4] Albrektsson, T, Dahlin, C, Jemt, T, Sennerby, L, Turri, A, Wennerberg, A, "Is Marginal Bone Loss around Oral Implants the Result of a Provoked Foreign Body Reaction?," Clin Implant Dent Relat Res. (2013), doi: 10.1111/cid.12142. Epub ahead of print
- [5] Yukna, RA, "Peri-implantitis Therapy with the LANAP® Protocol," American Academy of Periodontology 99<sup>th</sup> Annual Meeting, Corporate Forum, Philadelphia PA, (2013).
- [6] Charalampakis, G, Leonhardt, Å, Rabe, P, Dahlén, G, "Clinical and microbiological characteristics of peri-implantitis cases: a retrospective multicentre study," Clin Oral Implants Res, 23(9), 1045-54 (2012).
- [7] Roos-Jansåker, AM, Lindahl, C, Renvert, H, Renvert, S, "Nine- to fourteen-year follow-up of implant treatment. Part I: implant loss and associations to various factors," J Clin Periodontol, 33(4), 283-289 (2006).
- [8] Lindhe, J, Meyle, J, "Group D of European Workshop on Periodontology. Peri-implant diseases: Consensus Report of the Sixth European Workshop on Periodontology," J Clin Periodontol, 35(8 Suppl), 282-285 (2008).
- [9] Gregg, RH, McCarthy, DK, "Laser ENAP for periodontal bone regeneration," Dent Today, 17, 88-91 (1998).
- [10] Gregg, RH, McCarthy, DK, "Laser ENAP for periodontal ligament regeneration," Dent Today, 17, 86-88 (1998).
- [11] Gregg, RH, McCarthy, DK, "Laser periodontal therapy: case reports," Dent Today, 20, 74-81 (2001).
- [12] Gregg, RH, McCarthy, DK, "Laser periodontal therapy for bone regeneration," Dent Today, 21, 54-59 (2002).
- [13] Yukna RA, Evans GH, Vastardis S, and Carr, RL, "Human periodontal regeneration following the laser assisted new attachment procedure," Paper presented at: IADR/AADR/CADR 82nd General Session; March 10-13, 2004; Honolulu, HI. Abstract 2411.
- [14] Yukna RA, Carr RL, Evans GH, "Histologic evaluation of an Nd:YAG Laser-Assisted New Attachment Procedure in humans," International Journal of Periodontics & Restorative Dentistry 26, 577-587 (2007).
- [15] Nevins ML, Marcelo, C, Schupbach, P, Kim, S-W, Kim, DM, Nevins, M, "Human clinical and histologic evaluation of Laser-Assisted New Attachment Procedure. International Journal of Periodontics & Restorative Dentistry 32(5), 497-507 (2012).
- [16] Harris, DM and Jacques, SL, "Monte Carlo Simulation of depth of kill of *P. gingivalis* in dentin based on experimental damage threshold," Amer. Soc. Lasers Med. Surg. 25<sup>th</sup> Annual Conference, Orlando FL (2005).
- [17] Reinisch, L, "Scatter-limited phototherapy: a model for laser treatment of skin," Lasers Surg Med, 30(5), 381-388 (2002).



Figure 1. A case of peri-implantitis treated by LAPIP in a 44 year old female. Natural tooth #8 (a) was extracted and replaced with an implant (b) in 2004. In 2010 she presented with peri-implantitis (c) and was treated with LAPIP. The lesion is outlined in the lower panels. The baseline alveolar crest is identified at the time of implant (d). The clusters of green pixels represent pixels with a grey-level value that, in this case, defines the boundary criteria for the edge of the lesion. This case was provided by Dr. Finkbiener.

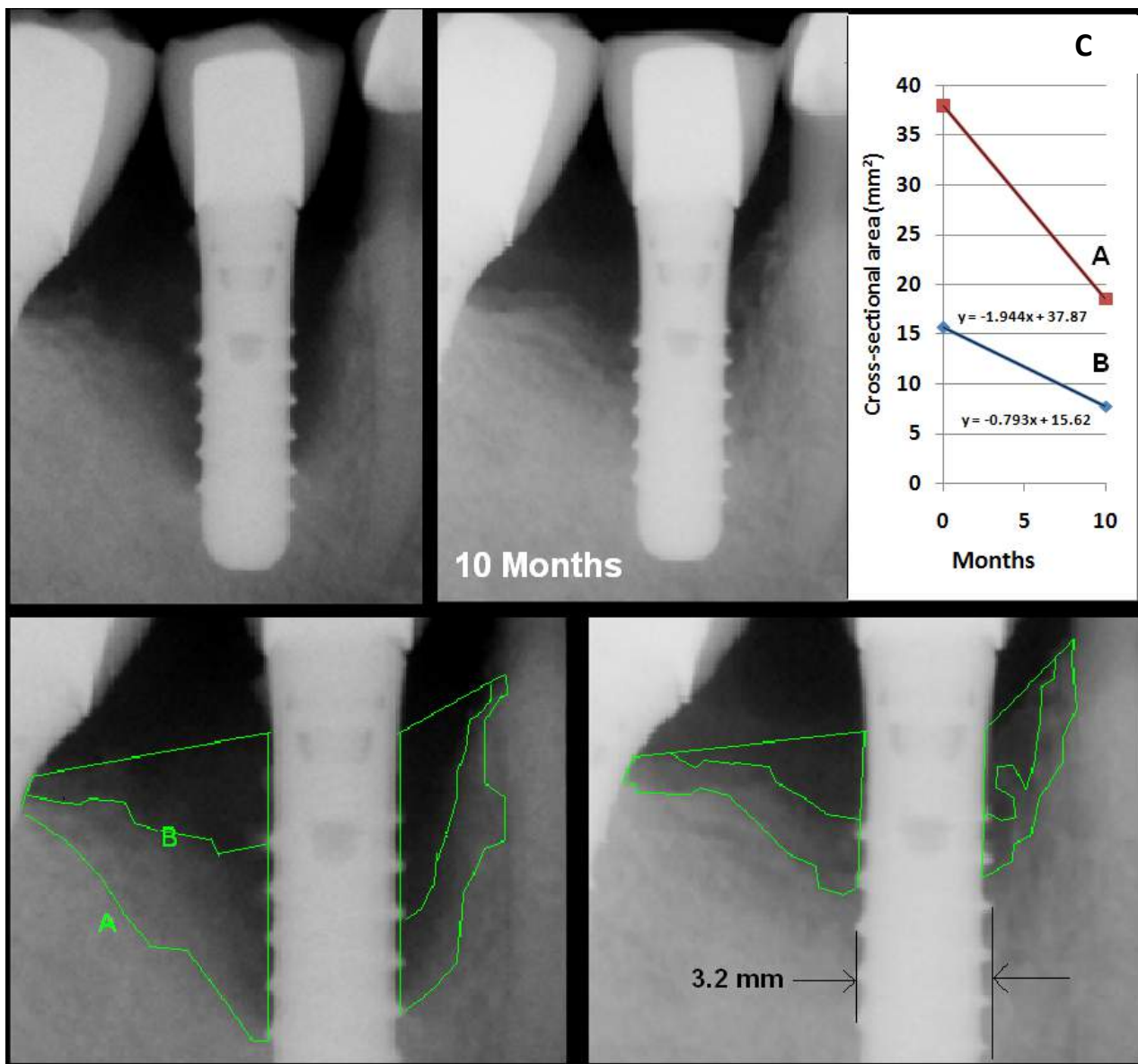


Figure 2. Case of peri-implantitis 3 years post-implant in a 51 year old male provided by Dr. Lamas. Two different contours are identified in these images. The “x-ray shadow” within the alveolar bone is assumed to represent bone loss resulting in decreased radiodensity (contour A). Completely black areas (there may be a slight of soft tissue background) are assumed to represent areas where bone is absent (contour B). C. The change in cross-sectional area was at a rate of 1.94 mm<sup>2</sup>/month for the entire lesion. The decrease in the black area (growth of new bone) was at a rate of 0.792 mm<sup>2</sup>/month [approx 1.6 mm<sup>3</sup>/mo].

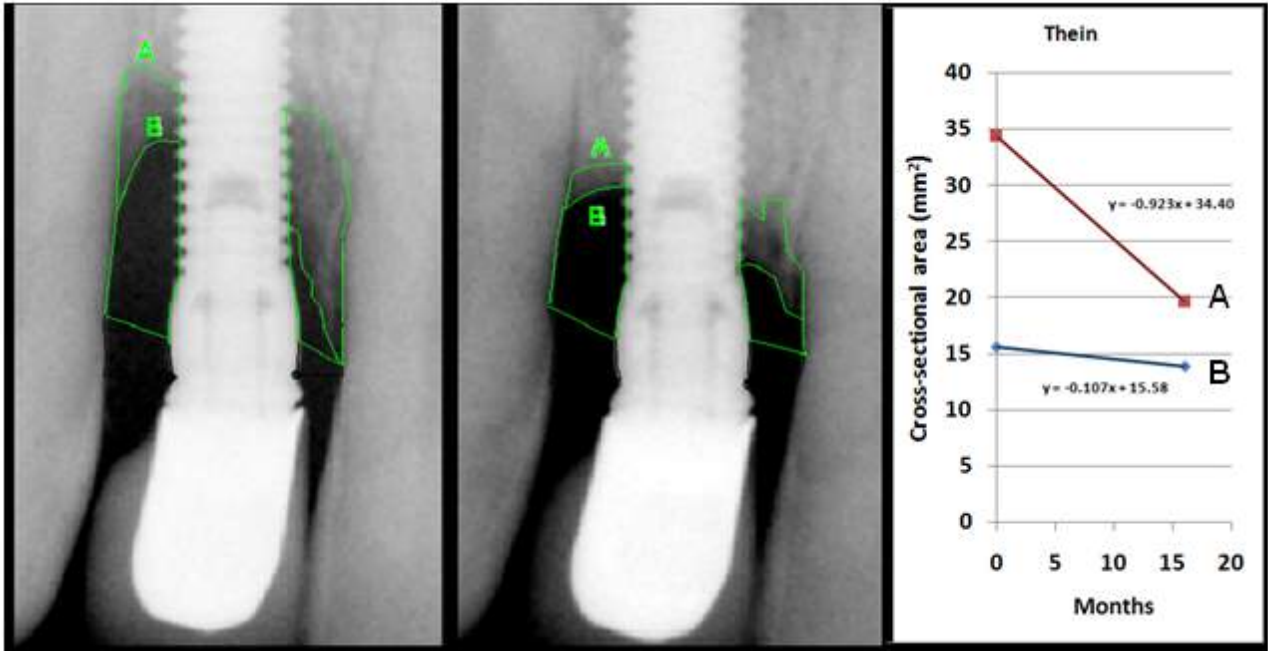


Figure 3. Case of peri-implantitis in a 55 year old female provided by Dr Thein. The two different contours are also evident in this case. The cross section of the entire lesion was  $34 \text{ mm}^2$  and receded at a rate of  $0.923 \text{ mm}^2/\text{month}$  with new bone deposited at a rate of  $0.107 \text{ mm}^2/\text{month}$  (approx.:  $0.620 \text{ mm}^3/\text{mo}$ ).



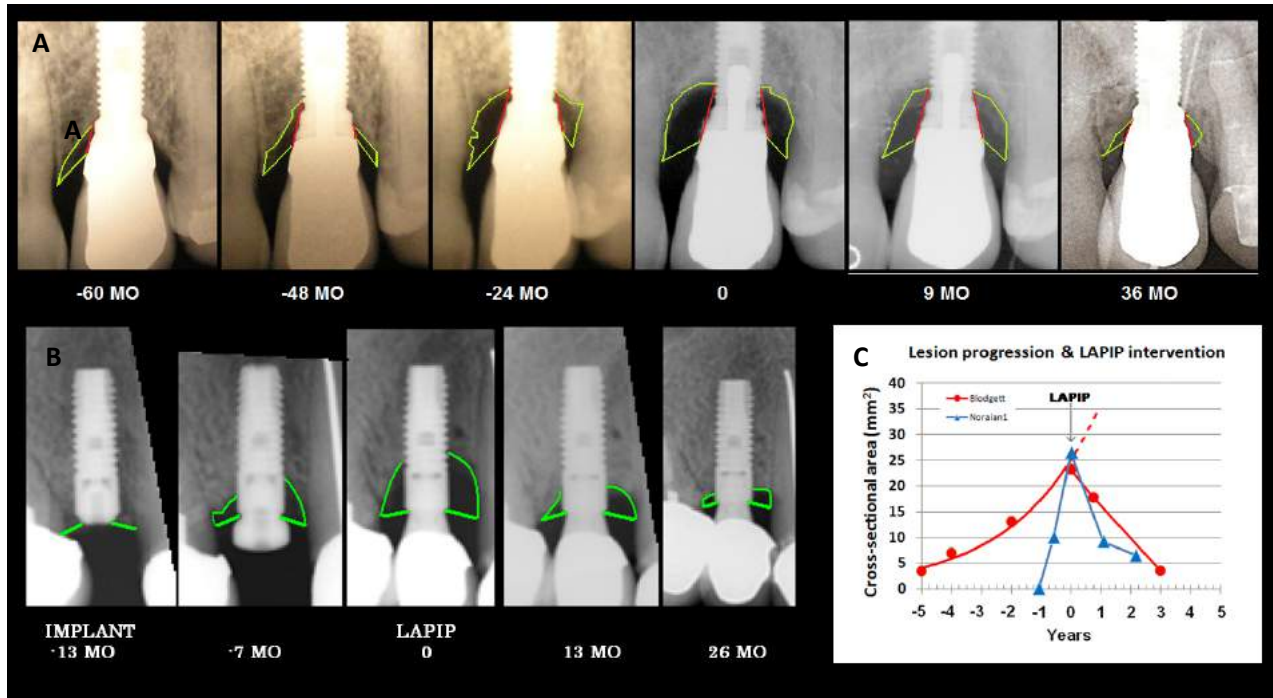


Figure 4. Lesion progression and LAPIP intervention. Two cases illustrating the development of the lesion and the response to LAPIP therapy.

A. A slow growing lesion that started to develop around the time of implant. LAPIP therapy had an immediate effect and the defect was resolved in three years. This case provided by Dr. Blodgett.

B. A radiograph from the time of implant (-13 Mo) provides a baseline for measuring bone loss in this rapidly progressing lesion. The immediate response to therapy is at a rate of 0.771 mm<sup>2</sup>/month. The 26-Mo image is foreshortened relative to the others and areas may be underestimated. This case was provided by Dr. Noraian.

C. The cross-sectional area of the lesion (right plus left) VS time shows an exponential lesion progression and an immediate and long lasting response to LAPIP intervention.

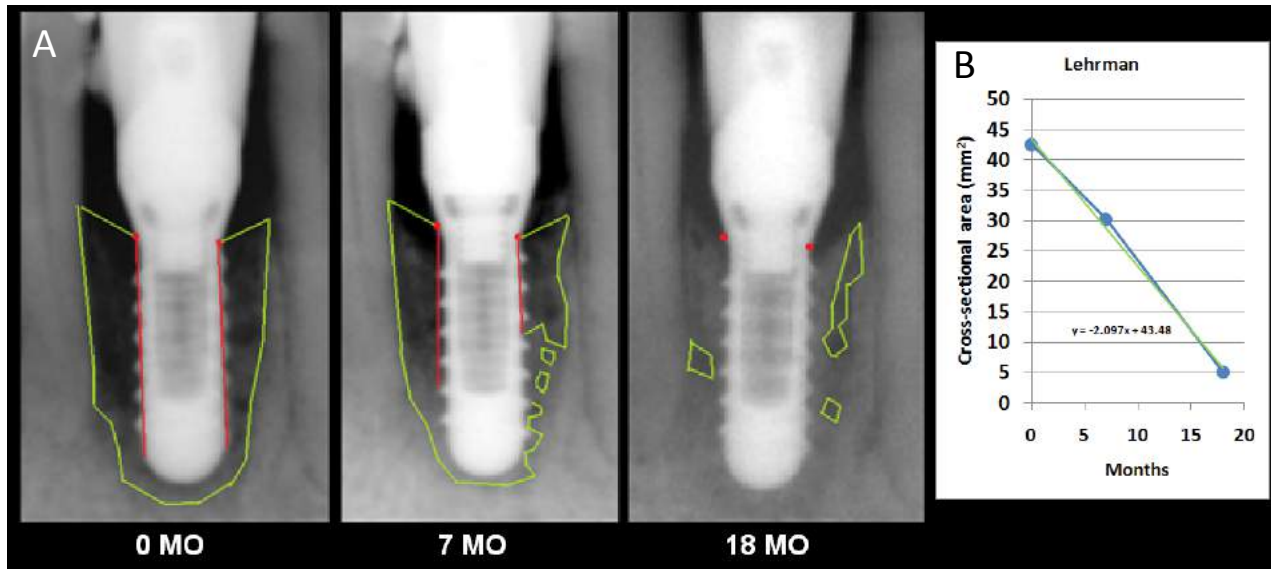


Figure 5. An “extraordinary” LAPIP case provided by Dr. Lehrman. 72 year old male with a four year old implant. (A) A large lesion (43 mm<sup>2</sup>) that encompassed the entire interdental space between tooth #23 and #25. One of the most rapid responding lesions. (B) Total lesion area measured with ImageJ VS time post-LAPIP. The linear regression indicates a rate of healing of 2.097 mm<sup>2</sup>/month. See text for more details.

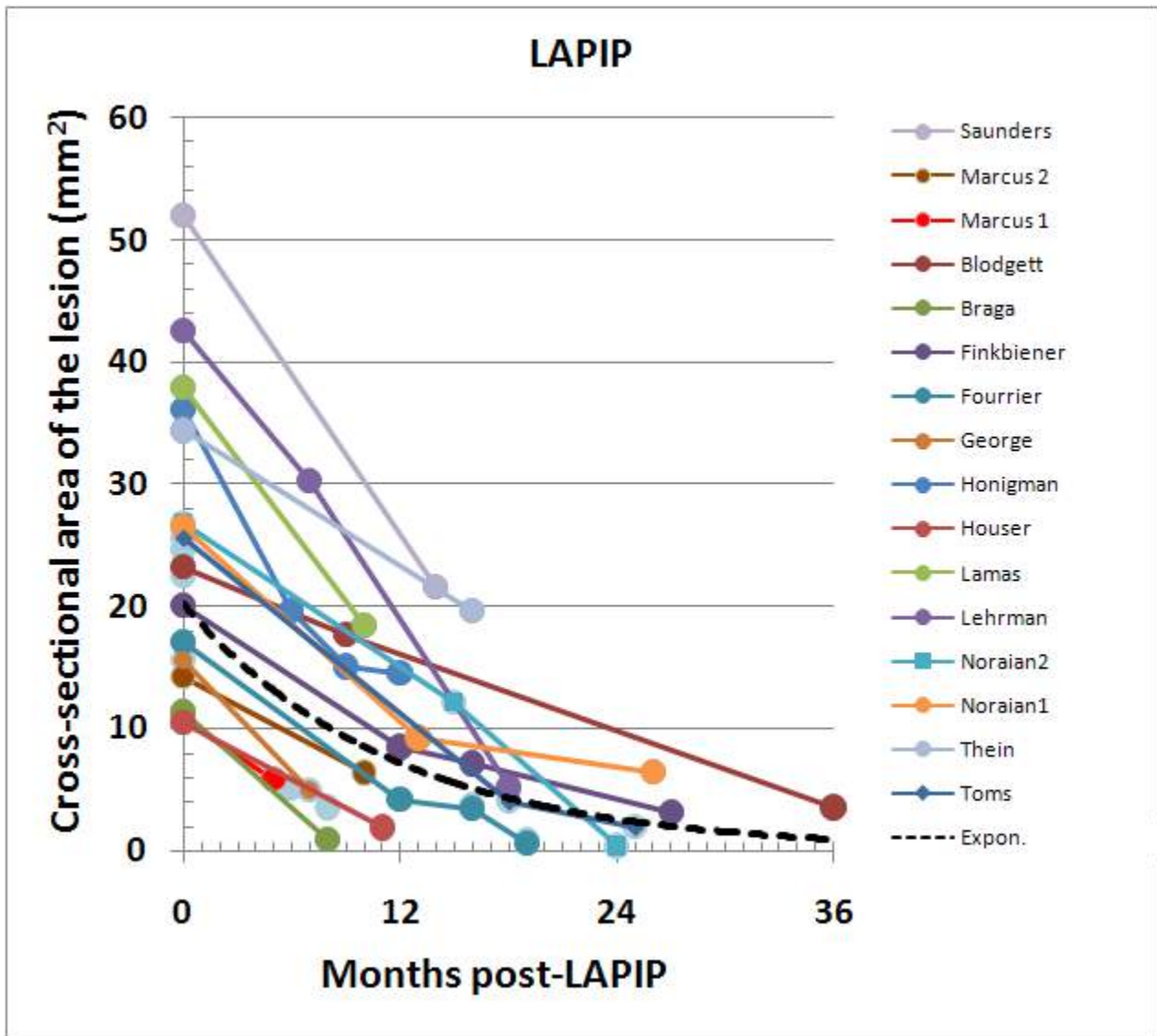


Figure 6. Recovery functions following LAPIP therapy. Plotted are the cross-sectional areas VS time of follow-up for all 16 cases. Cross-sectional areas are the total of right plus left areas. In those cases with multiple time points there is a trend for recovery to slow over time. Larger lesions appear to heal faster. Complete recovery takes from 1-3 years depending on the initial size of the lesion. The dotted line is an exponential fit to all data points and represents a characteristic healing curve. Average rate of recovery =  $14.9\text{mm}^2 / \text{year}$ .

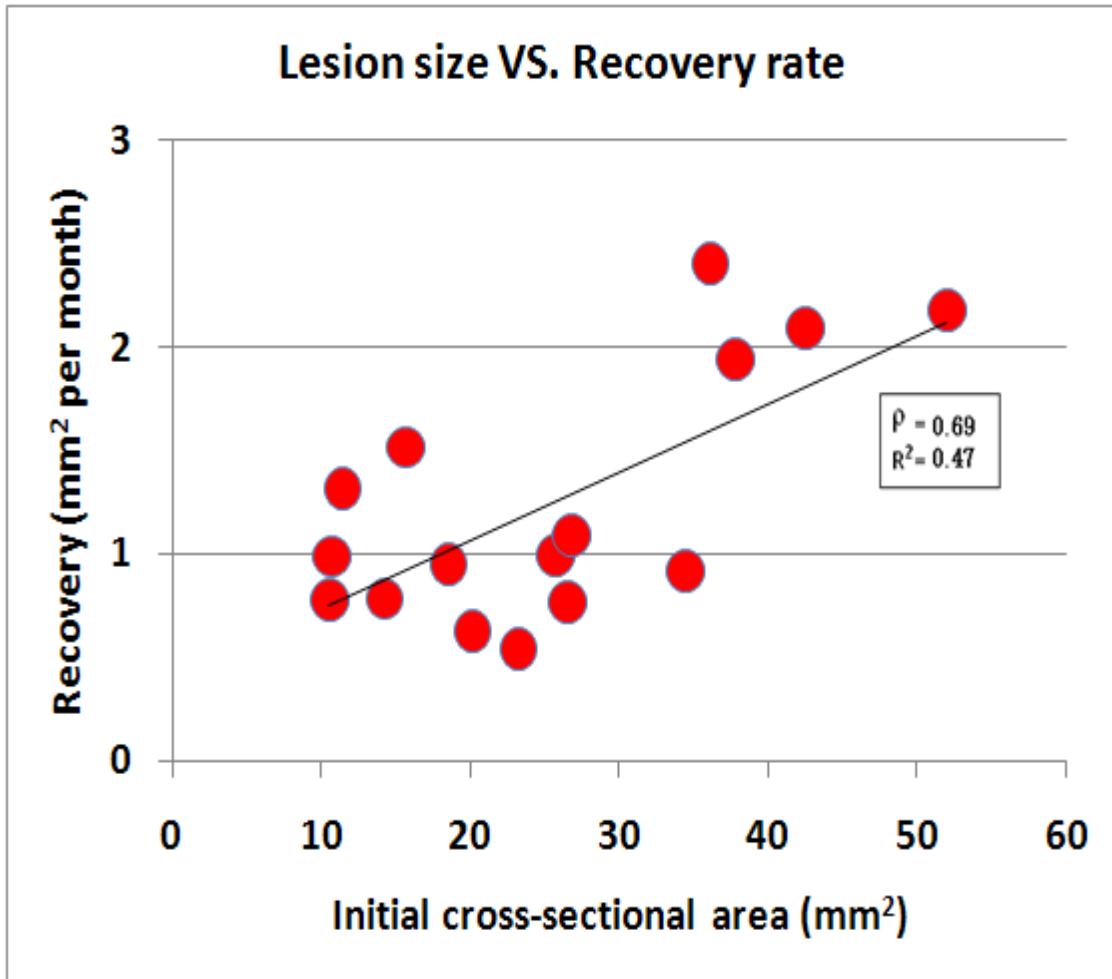


Figure 7. Initial lesion size VS recovery rate. There is a modest trend for larger lesions to heal more rapidly. Root mean square ( $R^2 = 0.47$ ), correlation coefficient ( $\rho = 0.69$ ).

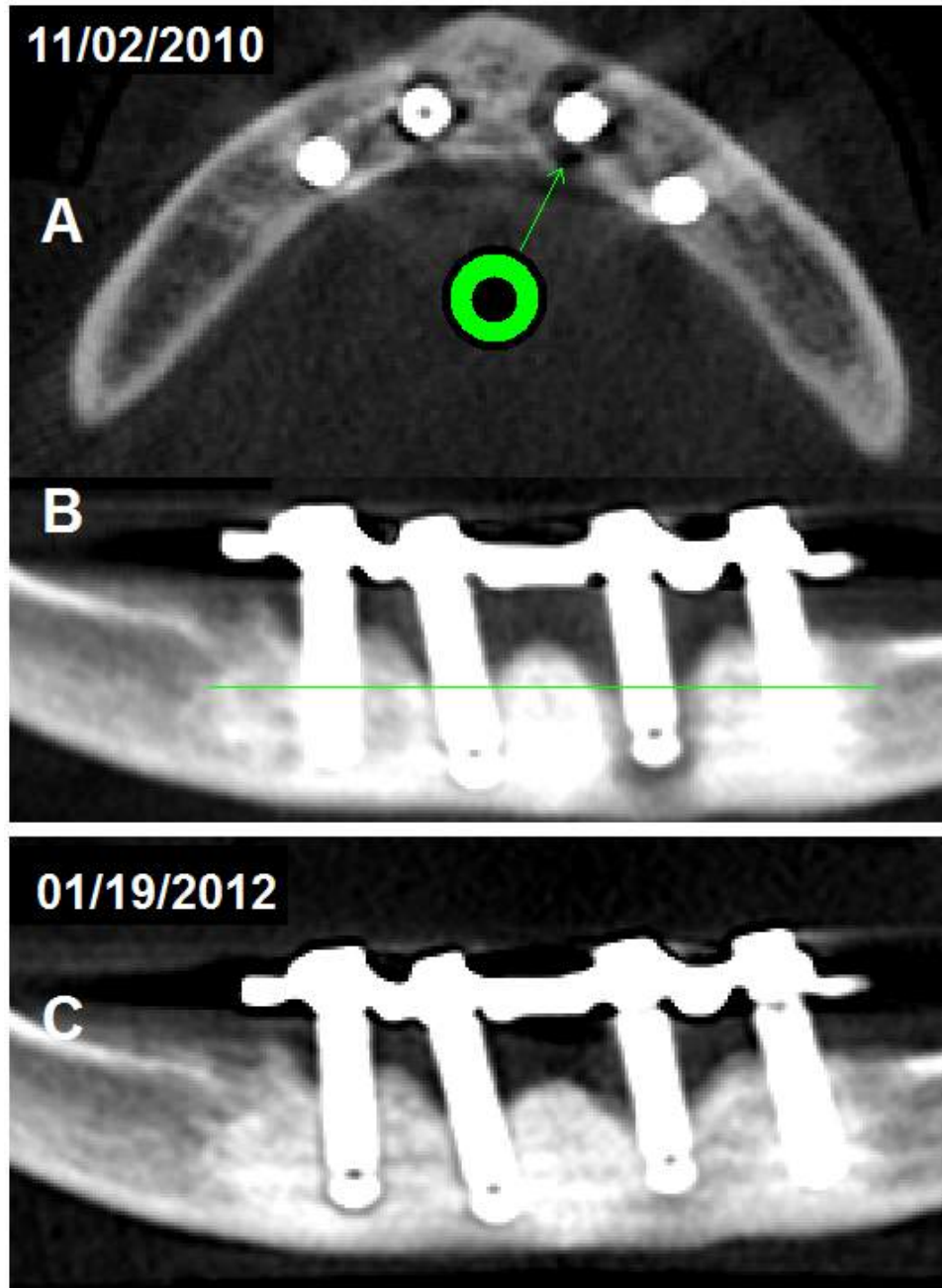


Figure 8. CT scan showing peri-implantitis in the anterior mandible of a 48 year old male.  
 A. Reconstruction of a horizontal section at about the level shown by the green line in B. Note the donut-shaped defect surrounding the implant.  
 B. Panoramic view. Radiolucency indicates total involvement including the apex of the implant (right) and partial involvement (left) at the time of treatment.  
 C. Reduction in area of radiolucencies by 14 months post-LAIP.  
 Case provided by Dr. Steven Saunders.

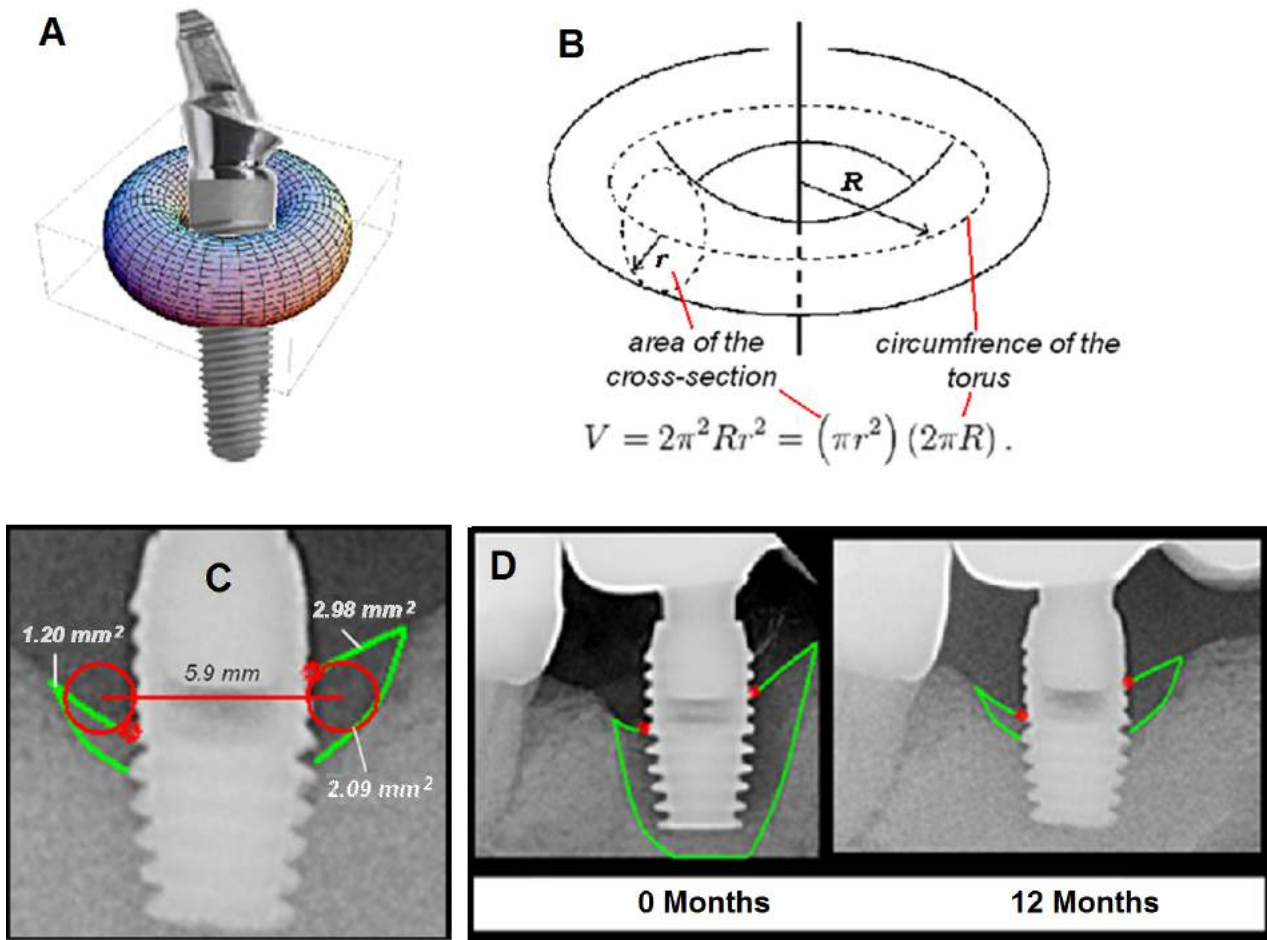


Figure 9. Geometric model used to estimate lesion volume.

A. Peri-implantitis is an infection that surrounds the neck of a dental implant. The 3-D shape is approximated by a torus.

B. The volume of a torus is equal to the circumference of the torus ( $2\pi R$ ) times its cross-sectional area ( $\pi r^2$ ).

C. For an actual lesion  $R = 2.95$  mm and the cross-sectional area, the average of right and left areas, =  $2.09$   $\text{mm}^2$ . The volume of this lesion at 12 months is estimated as  $38.7$   $\text{mm}^3$ .

D. Using the same approximation the initial volume of the lesion at 0 months was  $158$   $\text{mm}^3$ . Case provided by Dr. Fourrier.